Journal of Physiology (1993), **472**, *pp.* 341–357
With 5 figures
Printed in Great Britain

CALCIUM BUFFERING PROPERTIES OF CALBINDIN D_{28k} AND PARVALBUMIN IN RAT SENSORY NEURONES

BY PAUL S. CHARD*, DAVID BLEAKMAN*†, SYLVIA CHRISTAKOS‡, CURTIS S. FULLMER§ AND RICHARD J. MILLER*‖

*From the *Department of Pharmacological and Physiological Sciences, The University of Chicago, 947 East 58th Street, Chicago, IL 60637, the ‡Department of Biochemistry and Molecular Biology, New Jersey Medical School, Newark, NJ 07103, and the §New York State College of Veterinary Medicine, Cornell University, Ithaca, NY 14853-6401, USA*

(*Received 2 February 1993*)

SUMMARY

1. We have examined the ability of the Ca^{2+}-binding proteins (CABP) calbindin D_{28k} and parvalbumin to modulate increases in the intracellular free Ca^{2+} concentration ($[Ca^{2+}]_i$), produced by brief depolarizations, in rat dorsal root ganglion (DRG) neurones.

2. In order to obtain good voltage control, we replated DRG neurones prior to performing these experiments. Immunocytochemical staining of these cells revealed that approximately 10% stained for CABPs.

3. Using fluorescently labelled parvalbumin, we demonstrated that in the whole-cell voltage clamp mode the protein freely entered the cell soma with a mean half-life $t_{0.5}$ of 6 min 22 s ± 54 s.

4. Analysis of the effects of calbindin D_{28k} (370 μM) and parvalbumin (1 mM) on Ca^{2+} currents in the whole-cell voltage clamp mode, revealed that neither protein changed the rate of inactivation of the Ca^{2+} current or its rate of run-down.

5. Introducing either calbindin D_{28k} (370 μM) or parvalbumin (1 mM) into the cell soma did not significantly alter the basal $[Ca^{2+}]_i$ when compared to control cells.

6. Compared to control cells, both CABPs significantly reduced the peak $[Ca^{2+}]_i$ obtained for a Ca^{2+} influx of an equivalent charge density, whereas lysozyme (1 mM), a protein with low affinity for Ca^{2+}, failed to do so.

7. Calbindin D_{28k} caused an 8-fold decrease in the rate of rise in $[Ca^{2+}]_i$ and altered the kinetics of decay of $[Ca^{2+}]_i$ to a single slow component. Parvalbumin also slowed the rate of rise in $[Ca^{2+}]_i$. Parvalbumin selectively increased a fast component in the decay of the Ca^{2+} signal.

8. These data demonstrate that both calbindin D_{28k} and parvalbumin effectively buffer Ca^{2+} in a cellular environment and may therefore regulate Ca^{2+}-dependent aspects of neuronal function.

† Present address: Lilly Research Centre, Erl Wood Manor, Windlesham, Surrey GU20 6PH, UK.
‖ To whom correspondence should be addressed.

MS 2092

INTRODUCTION

Calbindin D_{28k} and parvalbumin belong to the EF-hand family of Ca^{2+}-binding proteins (Pochet, Lawson & Heizmann, 1990). The EF-hand, a Ca^{2+}-coordinating helix–loop–helix peptide sequence, was first described in the crystal structure of parvalbumin (Kretsinger & Nockolds, 1973) and has since been found in over twenty different groups of proteins including: calmodulin, troponin C, calretinin, calcineurin B and the S-100 proteins (Heizmann & Hunziker, 1991). Calbindin D_{28k} (28 kDa) has six EF-hand domains, of which two are non-functional, and thus binds Ca^{2+} with a stoichiometry of four. Parvalbumin (11 kDa) has two high affinity Ca^{2+}-binding domains, a third AB-domain being non-functional, and therefore binds Ca^{2+} with a stoichiometry of two. The EF-hand proteins can be thought of potentially as either 'sensors' or as Ca^{2+} buffers. The 'sensor' proteins behave primarily as regulators, affecting the activity of other proteins. An example of this is the regulation of protein kinases and other proteins by calmodulin. On the other hand, Ca^{2+} buffers are those EF-hand proteins whose primary function is thought to be binding of Ca^{2+} released into the cytoplasm. Calbindin D_{28k} and parvalbumin are currently thought to be Ca^{2+} buffers (Heizmann & Hunziker, 1991; Baimbridge, Celio & Rogers, 1992; Lledo, Somasundaram, Morton, Emson & Mason, 1992), although this property has never actually been demonstrated in neuronal cells.

Although it was first discovered in the gut (Wasserman & Taylor, 1966), calbindin D_{28k} is predominantly expressed in the central nervous system (CNS) where it shares a restricted, often complimentary, distribution with parvalbumin (Celio, 1990). The concentration of these proteins varies between cells, but in both cases has been estimated to be as high as 1 mM (Oberholtzer, Buettger, Summers & Matschinsky, 1988; Kosaka, Kosaka, Nakayama, Hunziker & Heizmann, 1993). In general, the exact physiological significance of these proteins remains unclear (Baimbridge *et al.* 1992). However, in fast twitch muscle it has been reported that there is a correlation between the parvalbumin concentration and the rate of relaxation of muscle fibres from contraction (Gillis, Thomason, Lefevre & Kretsinger, 1982; Hou, Johnson & Rall, 1991). In addition, in hippocampal neurones, there is a correlation between the presence or absence of calbindin D_{28k} and resistance to cell death following seizure activity (Sloviter, 1989; Leranth & Ribak, 1991), or following exposure to either Ca^{2+} ionophore or glutamate (Mattson, Rychlik, Chu & Christakos, 1991). It is assumed from data of this type that calbindin D_{28k} and parvalbumin exert these effects in neurones by buffering $[Ca^{2+}]_i$, although this remains to be demonstrated. In the present study we have used combined whole-cell patch clamp–fura-2 based microfluorimetry to introduce exogenous calbindin D_{28k} and parvalbumin into cultured DRG neurones in order to examine their Ca^{2+} buffering properties within a cellular environment.

Some of the preliminary findings have been reported to the Society for Neuroscience (Chard, Bleakman & Miller, 1991).

METHODS

Cell culture

Neurones were cultured from the dorsal root ganglia (DRG) of neonatal rats essentially as described previously (Thayer, Perney & Miller, 1988*a*). Briefly, DRG neurones, dissected from the

thoracic and lumbar segments of 3- to 5-day-old Holtzman rats, were incubated sequentially for 10 min at 37 °C in collagenase (0·1 %), collagenase–dispase (0·1 %) and trypsin (2·5 %). The digestion was halted by addition of equal volume of horse serum (4 °C) and subsequent centrifugation (5 min, 1000 r.p.m.). The ganglia were transferred to culture medium (4 °C) and dissociated into single cells by trituration through a Pasteur pipette. The cells were then plated on laminin–fibronectin-coated coverglasses (15 or 25 mm diameter) and incubated in Ham's medium mixture F-12 (Gibco, Grand Island, NY, USA) supplemented with 5 % heat-inactivated rat serum, 4 % 17-day embryonic extract, 50 ng ml^{-1} nerve growth factor, 44 mM glucose, 2 mM L-glutamine, 1 % Eagle's minimal essential medium 100 × vitamins and penicillin–streptomycin (100 μg ml^{-1} and 100 U ml^{-1} respectively) (Gibco) which was replaced every 2–3 days. Cultures were maintained at 37 °C in a water-saturated atmosphere with 5 % CO_2. Cells between 5 and 21 days *in vitro* were used for the present experiments.

To ensure good voltage clamp of DRG neurones, neuronal processes were removed by replating the cells 1 h before the experiment. Cells were replated as follows: cultured DRG neurones were transferred to a Ca^{2+}- and Mg^{2+}-free Hank's solution modified by the addition of 10 mM Hepes, 44 mM glucose, minimum essential (20 ml l^{-1}) amino acid and (10 ml l^{-1}) vitamin solutions (Gibco). Cells were dislodged from the coverslip and gently triturated using a Pasteur pipette. The isolated cells were replated onto laminin–fibronectin-coated glass coverslips and, after 2–3 min, Ca^{2+} and Mg^{2+} were added back to the media (approximately 500 and 250 μM, respectively). Neurones were then incubated for 1 h at 37 °C in a water-saturated atmosphere with 5 % CO_2. Cells which adhered to the coverslips were devoid of processes and were between 15 and 30 μm in diameter.

Whole-cell patch clamp

The tight seal whole-cell configuration of the patch clamp technique (Hamill, Marty, Neher, Sakmann & Sigworth, 1981) was used to record the transmembrane I_{Ca} from single cells while simultaneously measuring changes in $[Ca^{2+}]_i$. The methods used for this study have been described previously in detail (Thayer, Sturek & Miller, 1988*b*). Coverslips (25 mm diameter), with replated DRG neurones, were mounted in the perfusion chamber and continuously perfused with a buffer solution composed of (mM): 138 NaCl, 2 $CaCl_2$, 1 $MgCl_2$, 5 KCl, 10 4-(2-hydroxyethyl)-1-piperazineethanesulphonic acid (Hepes) and 10 glucose, adjusted to pH 7·4 with NaOH or when isolating for Ca^{2+} currents (mM): 140 TEACl, 2 $CaCl_2$, 1 $MgCl_2$, 10 Hepes and 10 glucose adjusted to pH 7·4 with CsOH. Voltage clamp experiments were performed in the above solution which was positioned on the opening of the microscope stage. A cell was approached with a fire-polished pipette containing a solution composed of (mM): 0·1 fura-2 pentapotassium salt, 135 CsCl, 1 $MgCl_2$, 10 Hepes, 14 diTris phosphocreatinine, 3·6 MgATP and 50 units ml^{-1} creatinine phosphokinase; adjusted to pH 7·1 with CsOH ± either 0·37 calbindin D_{28k}, 1 parvalbumin, 1 lysozyme or 2 1,2-bis-(*O*-aminophenoxy)ethane-*N*,*N*,*N*′,*N*′-tetraacetic acid (BAPTA). Background fluorescence was recorded after formation of a gigaseal but before breaking into the cell, thus accounting for fluorescence contributed by the fura-2 in the pipette. Since the pipette approached the cell from above, the objective was focused below the pipette near the middle of the cell, to minimize the pipette fluorescence. Full diffusion of the fura-2 into the cell occurred over a period of 3–5 min. Only cells in which the series resistance was $\leqslant 6$ MΩ (where series resistance is equivalent to the access resistance as defined by Pusch & Neher (1988)) and the mean basal $[Ca^{2+}]_i$ was $\leqslant 200$ nM were considered acceptable for recording. Currents were recorded by a List EPC-7 amplifier, filtered by an 8-pole low pass Bessel filter with a cut-off frequency of 200 Hz and stored on a computer used for the fluorescence data acquisition.

Calibration and analysis

Records were corrected for experimentally determined background values and the ratio of 340/380 nm fluorescence calculated off-line. Ratios were converted to free Ca^{2+} by the equation, $Ca^{2+} = K(r-R_{min})/(R_{max}-R)$ in which R is the 340/380 nm fluorescent ratio (Grynkiewicz, Poenie & Tsien, 1985). The maximum ratio (R_{max}), the minimum ratio (R_{min}) and the constant K, the product of the dissociation product for fura-2 and the ratio of the free and bound forms of the dye at 380 nm, were determined from a fit to a standard curve using the above equation with a non-linear least squares analysis computer program (Fabatio & Fabatio, 1979). The standard curve was determined for the fura-2 salt in calibration buffer (mM): 20 Hepes, 120 KCl, 5 NaCl, 1 $MgCl_2$, adjusted to pH 7·1; containing 10 mM ethylene glycol-bis-(β-aminoethylether)-*N*,*N*,*N*′,*N*′-tetra-acetic acid (EGTA), dissociation constant (K_d) = $3{\cdot}696 \times 10^{-6}$ M with calculated amounts of Ca^{2+} added to give free calcium concentrations ranging between approximately 0 and 2000 nM. Identical

calibration curves were obtained if CsCl was used to replace KCl. No change in the fura-2 isobestic point could be detected when excitation spectra were derived in the presence of 370 μM calbindin D_{28k}, 1 mM parvalbumin or 1 mM lysozyme and compared to control. Experiments performed over long periods of time (> 30 s) were digitally filtered with an algorithm which added half the value of each datum point to quarter of the value of each neighbouring point. The data were cycled through this routine 5 times. The $[Ca^{2+}]_i$ traces in patch clamp experiments were digitally filtered by a single cycle through an eleven point moving average algorithm.

Digital imaging experiments were performed essentially as described above using fluorescence imaging software (Universal Imaging Corp., PA), a model C2400 intensified CCD camera (Hamamatsu Corp., Hamamatsu City, Japan) and a model MVPAT Matrox frame grabber board (Matrox Electronic Systems Ltd, Quebec, Canada). Images were collected very 30 s, and each image was an average of 16 frames. Intensity values were derived from defined regions and were stored and monitored in real time.

Calcium-binding protein labelling

Parvalbumin was labelled according to the method of Kellog, Mitchison & Alberts (1988) with minor modifications. Briefly, 5 mg rabbit muscle parvalbumin was dissolved in 400 μl 100 mM $NaHCO_3$ at pH 8·4, and 1 mg lissamine rhodamine B sulphonyl chloride (*N*-[9-{4-(chlorosulphonyl)-2-sulphophenyl}-6-(diethylamino)-3(h)-*N*-ethyl-3-ylidene])-*N*-ethylhydroxide) was dissolved in 10 μl dimethylformamide (DMF). The two were mixed and stirred at 37 °C for 1 h in the dark. The solution was then applied to a 10 ml 10 DG disposable desalting column (Bio-rad Labs, Richmond, CA) and fractions were collected in 0·7–0·9 ml aliquots. The optical density (OD) of the fractions was measured at 575 nm. The fraction containing the highest concentration of protein was used in the electrophysiological experiments.

Immunocytochemistry

Immunocytochemistry adhered to the procedure provided in Vectastatin ABC kits (Vector Labs Inc., Burlingame, CA). DRG neurones were immunocytochemically stained using monoclonal anti-mouse antibodies directed against parvalbumin (Sigma Chemical Co., St Louis, MO) and polyclonal anti-rabbit antibodies directed against both calcium-binding proteins which were kindly provided by Dr K. Baimbridge (University of British Columbia, Vancouver, Canada). For each coverslip, cells in four adjacent fields were counted and the positively staining neurones were expressed as a fraction of the total neurones counted.

Materials

Fura-2 pentapotassium salt and lissamine rhodamine B sulphonyl chloride were obtained from Molecular Probes Inc. (OR, USA). Rabbit muscle parvalbumin was from Sigma Chemical Co.

RESULTS

Cultured dorsal root ganglion (DRG) neurones extend long neuronal processes which, by virtue of their presence, make it difficult to obtain good voltage control during experimental recordings. To obviate this problem, we dislodged the DRG neurones by gentle trituration and replated them onto coverslips 1 h prior to the start of the experiment (see Methods for details). This simple procedure allowed for good voltage control in all cells examined ($n = 154$ cells).

Before introducing Ca^{2+}-binding proteins (CABPs) into DRG neurones, we first characterized the cultured neurones for endogenous CABP content. Cells were stained immunocytochemically with polyclonal anti-rabbit or monoclonal anti-mouse antibodies directed against either calbindin D_{28k} or parvalbumin. Approximately $18·5 \pm 1·6\%$ ($n = 10$ coverslips) of cultured DRG neurones were immunoreactive for calbindin D_{28k} while $10·1 \pm 2·0\%$ ($n = 15$ coverslips) were immunoreactive for parvalbumin. However, immunocytochemical staining performed on the replated neurones (1 h after replating) revealed differing levels of

CABP immunoreactivity. Parvalbumin immunoreactivity was reduced to $0{\cdot}7 \pm 0{\cdot}7$ % ($n = 11$) while calbindin D_{28k} immunoreactivity was reduced to $10{\cdot}3 \pm 3{\cdot}1$ % ($n = 7$). The intensity of staining was also reduced in the replated neurones. Thus, at the outset of our experiments, approximately 10 % of the neurones were immunoreactive for the two CABPs.

Introduction of CABPs into neurones was achieved by adding them to the intracellular solution in the patch pipette and allowing them to diffuse into the neurone in the whole-cell configuration. Prior to undertaking the investigation, we felt it was necessary to demonstrate that CABPs added to the patch pipette actually accessed the cell soma. In order to address this question, we covalently labelled parvalbumin with the fluorophore lissamine rhodamine B. Labelled parvalbumin was added to the patch pipette; individual DRG neurones were voltage clamped at $V_h = -80$ mV (holding potential); and the time course of the increase in cell fluorescence was monitored at 590 nm by either digital imaging or microfluorimetry. Half-maximal fluorescence occurred between 3 and 9 min (mean $t_{0{\cdot}5} = 6$ min 22 s $\pm$ 54 s, $n = 5$) and generally reached a maximum value at about 9–18 min. Figure 1 shows typical images taken at various times after achieving the whole-cell configuration for an individual DRG neurone. The bottom right graph compares the time course of unbound lissamine rhodamine B diffusion with that of the labelled protein. The time course for unbound lissamine rhodamine B was similar to that observed for fura-2 pentapotassium salt and was maximal after 3–5 min. Since it was clear that CABPs could access the cell soma, we added CABPs to the intracellular solution in the presence of 100 μM fura-2 salt and monitored their effects on $[Ca^{2+}]_i$.

The CABPs appeared not to interfere with fura-2 emission since the fura-2 isobestic point obtained in the presence of either 370 μM calbindin D_{28k} or 1 mM parvalbumin resulted in the same isobestic point as that determined for control solutions (data not shown). Introducing calbindin D_{28k} or parvalbumin into DRG neurones did not significantly alter the mean basal $[Ca^{2+}]_i$ during the time course of the experiment (up to 22 cells per time point), nor was there a significant difference between the mean basal $[Ca^{2+}]_i$ of control cells and of cells containing CABPs. Furthermore, in both cases, no correlation could be drawn between the resting basal $[Ca^{2+}]_i$ value and the magnitude of the peak $[Ca^{2+}]_i$ achieved in response to a depolarizing stimulus ($n = 67$ cells examined). Analysis of the rate of Ca^{2+} current inactivation revealed no significant difference in the rate of inactivation between control cells and cells containing either calbindin D_{28k} or parvalbumin (data not shown). Previous studies which have examined properties of neuronal Ca^{2+} currents without simultaneously monitoring $[Ca^{2+}]_i$ have routinely employed the high affinity Ca^{2+} chelator 1,2-bis(*O*-aminophenoxy)ethane-*N*,*N*,*N*′,*N*′-tetraacetic acid (BAPTA) in order to reduce the rate of 'run-down' of the currents. This time- and use-dependent reduction in the magnitude of the Ca^{2+} current is attenuated by addition of BAPTA to the patch pipette (Jones & Marks, 1989). In contrast, at the concentrations employed, neither calbindin D_{28k} or parvalbumin had any significant effect on the peak amplitude of the Ca^{2+} current or the rate of 'run-down' of evoked Ca^{2+} currents in the neurones examined (up to 13 cells per time point).

Although CABPs produced no effects on the basal $[Ca^{2+}]_i$ or on the rate of 'run-down' of Ca^{2+} currents, clear effects could be observed on the peak $[Ca^{2+}]_i$ achieved

in response to a depolarizing voltage step. Figure 2 (left side) shows typical data from three individual cells recorded from the same coverslip. A series of data sweeps (4 s duration) are shown taken at various times during the recording. Each time point refers to the time after gaining access to the cell. The cells were held at $V_h = -80$ mV

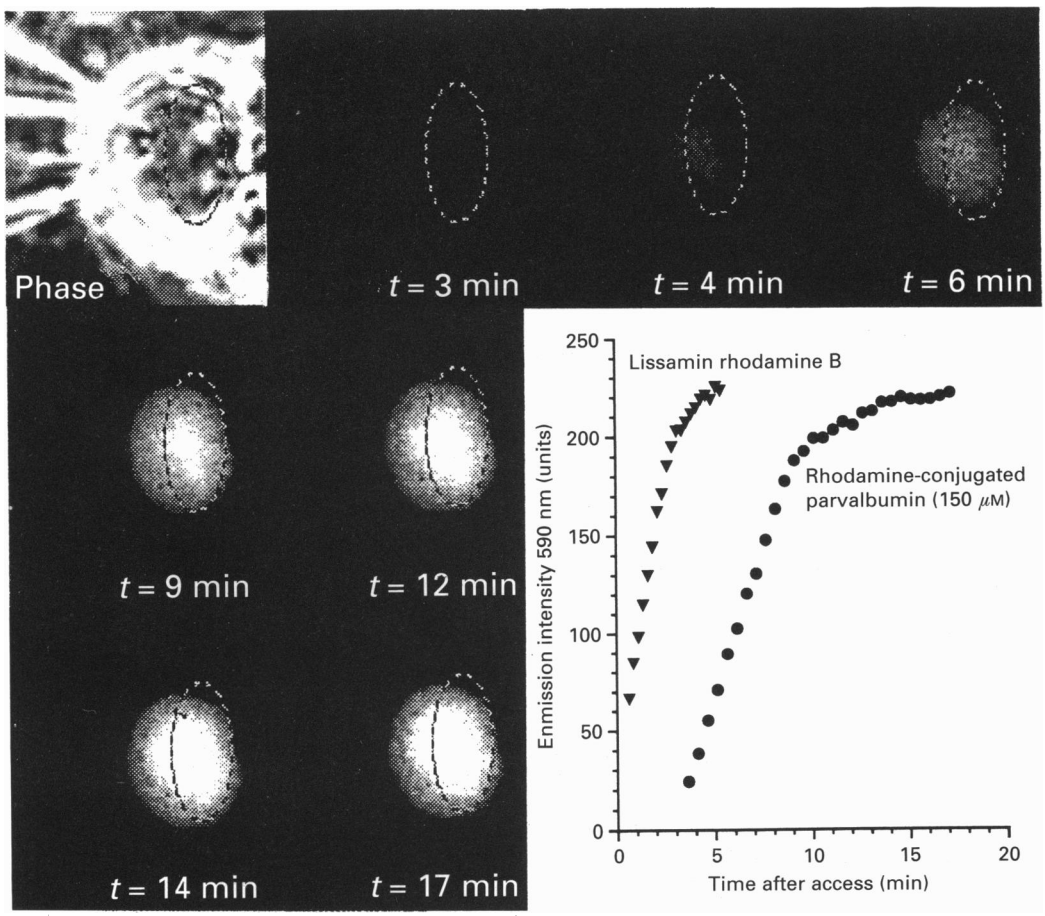

Fig. 1. Digital imaging of rhodamine-labelled parvalbumin diffusing into the cell soma of a single DRG neurone in the whole-cell patch clamp configuration. Rhodamine-labelled parvalbumin was added to the patch pipette and, under whole-cell voltage clamp ($V_h = -80$ mV), the time-dependent increase in cell fluorescence was monitored at 590 nm. Each panel represents an average of 16 frames, sampled at the times indicated. The time represents the time after gaining whole-cell access. Bottom right graph compares the time course of lissamine rhodamine B diffusion into an individual cell with that of the labelled protein into the cell shown in the images. $t_{\frac{1}{2}}$ maximal fluorescence = 6 min 22 s ± 54 s ($n = 5$).

(holding potential) and were depolarized to $V_t = 0$ mV (test potential) for 80 ms. The depolarizing step caused an inward Ca^{2+} current (seen as a downward deflection) and a concomitant rise in $[Ca^{2+}]_i$. It may be seen that cells which contained either calbindin D_{28k} or parvalbumin had smaller increases in $[Ca^{2+}]_i$ for similar sized peak

inward Ca^{2+} currents. Data derived from control and test cells were compared by first normalizing the $\Delta[Ca^{2+}]_i$ (peak–basal) for charge density (total charge influx per unit cell surface area). In order to rule out variations in culture and recording conditions as the underlying cause of the observed differences between control and test cells, the

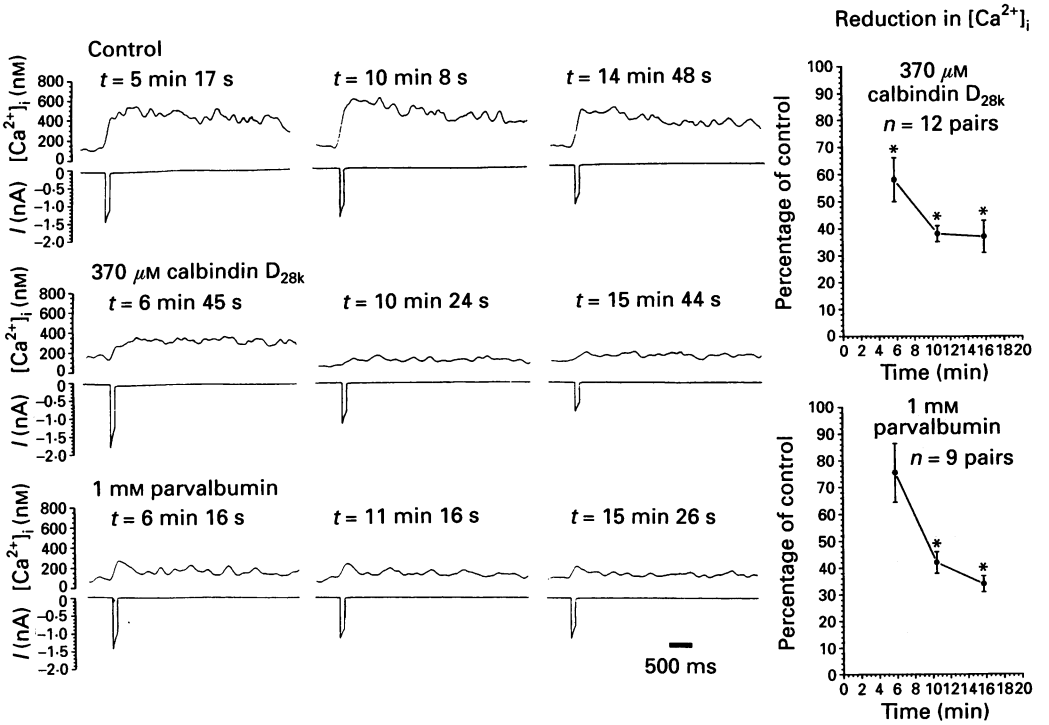

Fig. 2. Both calbindin D_{28k} and parvalbumin buffer the peak $[Ca^{2+}]_i$ achieved as a consequence of depolarization. The left-hand panels show a series of sweeps of data (each 4 s duration) taken at various time points during a recording from individual cells (t = time after gaining whole-cell access). Cells were held at $V_h = -80$ mV (holding potential) and depolarized to $V_t = 0$ mV (test potential) for 80 ms. The depolarizing step caused an inward current (seen as a downward deflection) and a concomitant rise in $[Ca^{2+}]_i$. During the time course of the experiment it can be seen that the cells containing either calbindin D_{28k} or parvalbumin had a smaller peak $[Ca^{2+}]_i$ for a similar peak I_{Ca}. The right-hand panels show graphs of the mean data for control and test cells recorded from the same coverslip. In order to control for variation between cells, the $\Delta[Ca^{2+}]_i$ (peak–basal) was normalized to charge density (total charge-influx per cell surface area). For each time point, the test cell has been expressed as a percentage of control. Vertical error bars represent the means ± S.E.M. Horizontal error bars are within the data point and represent the means ± S.E.M. of the individual sampling times. $*P < 0.001$, Student's paired t test.

normalized changes in $[Ca^{2+}]_i$ were only compared between recordings from control and test experiments performed on the same day. The paired data were then expressed as a percentage of control $\Delta[Ca^{2+}]_i$. Figure 2 (right side) shows the normalized mean data and reveals that the $\Delta[Ca^{2+}]_i$ compared to control cells became smaller over time, presumably as a consequence of the CABPs diffusing into

the cell, and was eventually reduced to $37 \pm 6\%$ ($P < 0{\cdot}001$, $n = 12$ pairs) and $34 \pm 3\%$ ($P < 0{\cdot}001$, $n = 9$ pairs) of control levels of calbindin D_{28k} and parvalbumin respectively. Interestingly, the time course of the decrease in $\Delta[Ca^{2+}]_i$ paralleled that of labelled parvalbumin influx into DRG neurones (Fig. 1). To investigate the

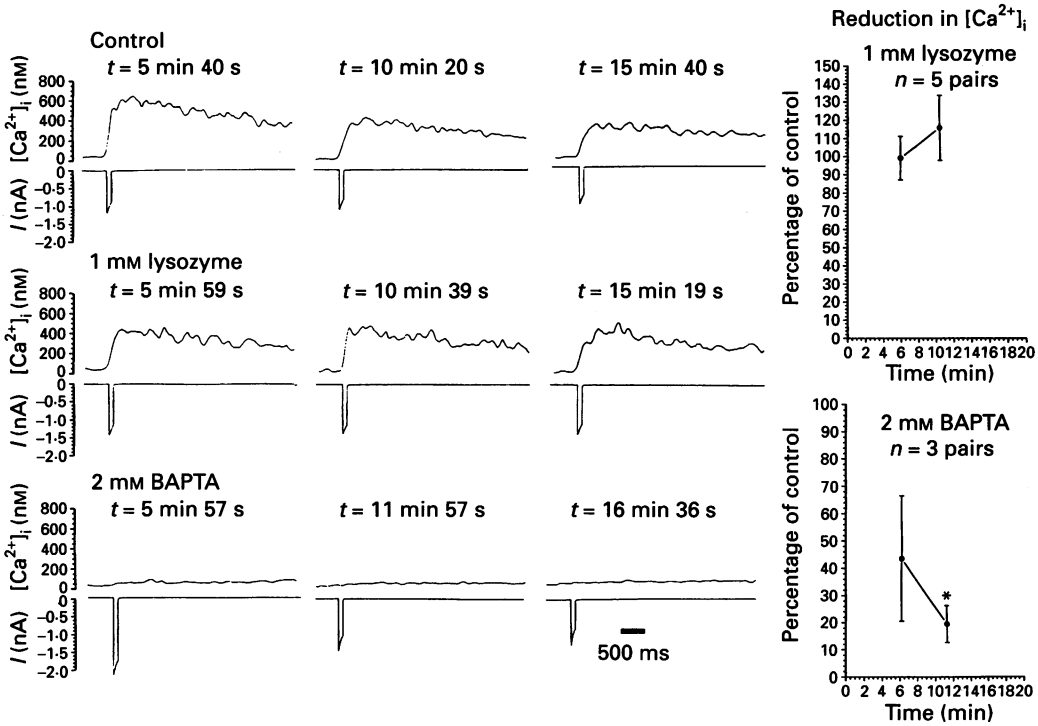

Fig. 3. 2 mM BAPTA buffers the peak $[Ca^{2+}]_i$ achieved as a consequence of depolarization in a manner analogous to the CABPs, whereas 1 mM lysozyme is without effect. The left-hand panels show a series of sweeps of data (each 4 s duration) taken at various time points during a recording from individual cells (t = time after gaining whole-cell access). Cells were held at $V_h = -80$ mV (holding potential) and depolarized to $V_t = 0$ mV (test potential) for 80 ms. The depolarizing step caused an inward current (seen as a downward deflection) and a concomitant rise in $[Ca^{2+}]_i$. During the time course of the experiment it can be seen that in contrast to the cell containing lysozyme the cell containing 2 mM BAPTA mimics the effect of the CABPs. The right-hand panels show graphs of the mean data for control and test cells recorded from the same coverslip. In order to control for variation between cells, the $\Delta[Ca^{2+}]_i$ (peak–basal) was normalized to charge density (total charge influx per cell surface area). For each time point, the test cell has been expressed as a percentage of control. Vertical error bars represent the means ± S.E.M. Horizontal error bars are within the data point and represent the means ± S.E.M. of the individual sampling times. *$P < 0{\cdot}05$, Student's paired t test.

possibility that the observed effect was artifactual, due to the introduction of protein *per se* into the cell rather than a consequence of Ca^{2+} buffering by the CABPs, we introduced 1 mM lysozyme into the patch pipette (Fig. 3). Lysozyme (12 kDa) is a similarly sized protein to parvalbumin (11 kDa) but does not bind Ca^{2+} efficiently. It can be seen that introduction of lysozyme into the cell soma had no significant effect

on the depolarization-induced increases in $[Ca^{2+}]_i$ (116·4 ± 18·1 % of control values, $n = 5$ pairs). In contrast, introduction of the high affinity Ca^{2+} chelator BAPTA mimicked the effect of the CABPs (19·3 ± 16·8 % of control values, $n = 3$ pairs) (Fig. 3).

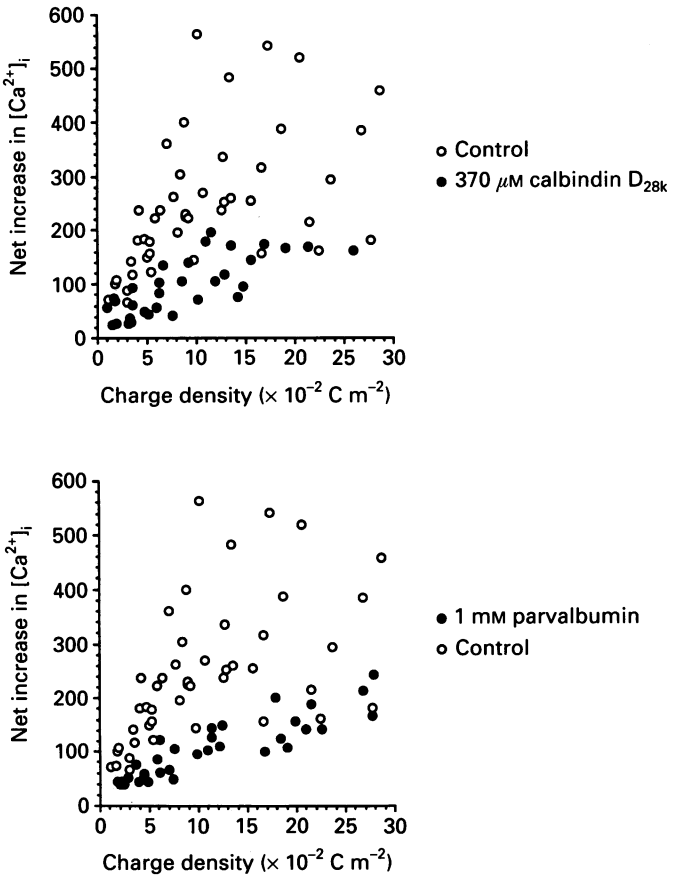

Fig. 4. Cells containing either calbindin D_{28k} or parvalbumin resist changes in $[Ca^{2+}]_i$ even for large Ca^{2+} challenges. Scatter plots compare the relationship between charge density and $\Delta[Ca^{2+}]_i$ (peak–basal) between control cells and cells containing either 1 mM parvalbumin or 370 μM calbindin D_{28k}. Cells voltage clamped at $V_h = -80$ mV (holding potential) were depolarized to $V_t = 0$ mV (test potential) for varying durations (40–1280 ms) and the evoked increases in $[Ca^{2+}]_i$ were measured. When compared to control cells, both calbindin D_{28k} (upper) and parvalbumin (lower) reduced the $\Delta[Ca^{2+}]_i$ throughout the range of charge density. Data were taken only from neurones in which 5 differing depolarizing steps were evoked (40, 80, 320, 640 and 1280 ms) at $t > 12$ min (following whole-cell access) during an experiment. Control data are derived from 9 cells, parvalbumin from 7 cells and calbindin D_{28k} from 9 cells.

We next examined whether the CABPs could buffer Ca^{2+} loads of increasing magnitude. Using control and test cells in which whole-cell access had been achieved for at least 12 min, we investigated their $[Ca^{2+}]_i$ over a range of Ca^{2+} challenges by

varying the depolarizing pulse duration between 40 and 1280 ms and examining the resulting $\Delta[Ca^{2+}]_i$. Figure 4 shows the relationship between charge density (total charge influx per unit cell surface area) and the resulting $\Delta[Ca^{2+}]_i$ for control cells and cells containing either calbindin D_{28k} or parvalbumin. It can be seen that for

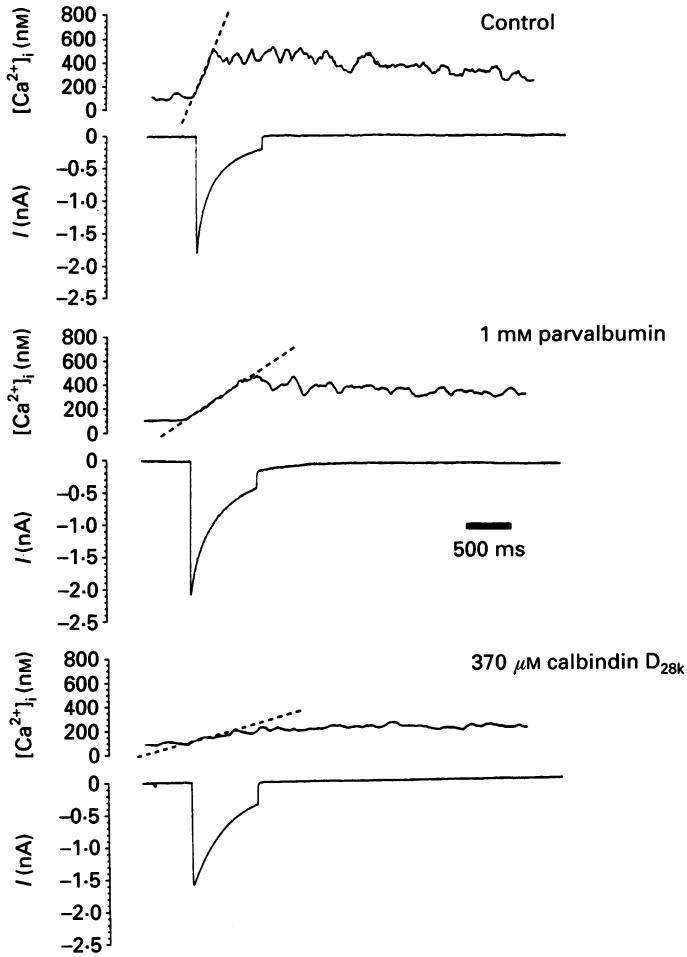

Fig. 5. 370 μM calbindin D_{28k} is 4-fold more effective than 1 mM parvalbumin in slowing the rate of rise in $[Ca^{2+}]_i$. Individual traces demonstrating the effect of introducing either 1 mM parvalbumin or 370 μM calbindin D_{28k} into DRG neurones on the rate of rise in $[Ca^{2+}]_i$ in response to a depolarizing voltage step from $V_h = -80$ mV (holding potential) to $V_t = 0$ mV (test potential) for a duration of 640 ms. Individual sweeps shown are representative of the mean data (see Table 1).

control cells there was a steep relationship between charge density and $\Delta[Ca^{2+}]_i$ while cells which contained either calbindin D_{28k} or parvalbumin produced consistently smaller increases in $[Ca^{2+}]_i$ for large Ca^{2+} loads.

Both CABPs reduced the peak $[Ca^{2+}]_i$ achieved as a consequence of depolarization. From a Ca^{2+}-signalling perspective at least two other parameters are of interest: the

rate at which the peak $[Ca^{2+}]_i$ is achieved and the rate at which the Ca^{2+} signal decays again. Figure 5 shows typical rates of rise in $[Ca^{2+}]_i$ ($d[Ca^{2+}]_i/dt$) for a 640 ms depolarizing pulse for three individual cells. Table 1 shows the mean data and reveals that the initial rate of rise in $[Ca^{2+}]_i$ (during the first 140 ms) when normalized to charge-influx during that time period was significantly slower for cells containing

TABLE 1. Both parvalbumin and calbindin D_{28k} display significantly slower rates of rise in $[Ca^{2+}]_i$ when compared to control

	Basal $[Ca^{2+}]_i$ (nM)	Peak current (nA)	Charge influx (during 1st 140 ms of sweep) (pC)	Rate of rise of $[Ca^{2+}]_i$ (during 1st 140 ms of sweep) (nM ms^{-1})	Rate of rise of $[Ca^{2+}]_i$ per picocoulomb (during 1st 140 ms of sweep) (nM s^{-1} pC^{-1})
Control ($n = 9$)	149 ± 14	1·23 ± 0·21	132 ± 26	2·18 ± 0·50	18·52 ± 3·42
Parvalbumin ($n = 8$)	146 ± 9	1·11 ± 0·20	119 ± 23	0·98 ± 0·17*	9·30 ± 1·27*
Calbindin ($n = 9$)	150 ± 12	1·33 ± 0·15	141 ± 17	0·29 ± 0·05†	2·40 ± 0·63†

Mean parameters for the initial rate of rise in $[Ca^{2+}]_i$ (measured over the first 140 ms of a 640 ms depolarizing step from $V_h = -80$ mV to $V_t = 0$ mV) are presented. In order to control for the effects of variations in the size of the peak current on the rate of rise in $[Ca^{2+}]_i$, we analysed the initial rate of rise over the initial 140 ms of the depolarizing step and normalized the rate to the total charge-influx occurring during that time. After normalizing the data, the rate of rise in $[Ca^{2+}]_i$ remained significant for both parvalbumin and calbindin D_{28k}. *$P < 0·05$, †$P < 0·001$, Student's unpaired t test.

CABPs. This effect was most pronounced in cells containing calbindin D_{28k} and is approximately 8-fold slower when compared to control cells ($P < 0·001$, $n = 9$). In order to assess the rate of decay of the peak Ca^{2+} signal, we compared cells in which the peak $[Ca^{2+}]_i$ value achieved was 300 ± 10 nM ($n = 7$) for control cells, 290 ± 3 nM ($n = 7$) for parvalbumin-containing cells and 299 ± 13 nM ($n = 9$) for calbindin D_{28k}-containing cells. Cells with similar peak $[Ca^{2+}]_i$ values were compared in order to rule out contaminating contributions of other buffering processes which might be recruited depending upon the $[Ca^{2+}]_i$ level (Thayer & Miller, 1990). In parvalbumin-containing cells there appeared to be a characteristic biphasic decay of the Ca^{2+} signal (see Fig. 2). A very rapid initial decay in which the time to decay to 80% of its initial value ($t_{0·8}$) was significantly quicker than in control cells (0·15 ± 0·04 s *vs.* 0·42 ± 0·10 s respectively, $P < 0·05$, $n = 7$) followed by a slower second phase ($t_{0·5}$) for parvalbumin *vs.* control; 1·16 ± 0·36 s *vs.* 1·94 ± 0·20 s, $n = 7$). This decay pattern was most clearly observed in response to shorter depolarizing pulse durations. In calbindin D_{28k}-containing cells (see also Fig. 2), a different decay pattern was observed characterized by a loss of the fast component of decay and appearing as a monophasic decay from peak $[Ca^{2+}]_i$ which was significantly slower than that observed for control cells ($t_{0·8}$ calbindin D_{28k} *vs.* control; 2·23 ± 0·41 s *vs.* 0·42 ± 0·10 s, $P < 0·001$, $n = 9$).

DISCUSSION

Calbindin D_{28k} and parvalbumin have frequently been localized to distinct subpopulations within the CNS and are often used as markers of cell types (Celio, 1990). However, at present it is still unclear whether CABPs are markers of cell morphology, cell function or both. Indeed, in the case of adult DRG neurones no correlation between morphology or modality and the presence or absence of CABPs has been made (Carr, Yamamoto, Karmy, Baimbridge & Nagy, 1989). The percentage of endogenous calbindin D_{28k} and parvalbumin immunoreactivity (22 and 14% respectively) in the adult ganglia correlated well with the percentage observed in the cultured neonatal DRG neurones used in our experiments (18 and 10% respectively). The loss of immunoreactivity upon replating may be due to the CABPs washing out from the cell during the replating process. However, we cannot rule out the possibility that these CABP-containing neurones are selectively lost during the replating process. In the whole-cell configuration, the residual CABP, observed in 10% of the cells after replating, will have been infinitely diluted upon equilibration with the contents of the patch pipette and thus was unlikely to have affected our results.

Labelled parvalbumin accessed the cell soma with a $t_{0.5} = 6$ min 22 s in good agreement with the theoretical diffusion time for exchange between pipette and cytoplasm determined by Pusch & Neher (1988). According to their calculations, with an average access resistance of 6 MΩ and average cell radius of 10·8 μm, parvalbumin (11 kDa) and calbindin D_{28k} (28 kDa) would have time constants of 3·7 and 5·0 min respectively. Furthermore, the theoretical and observed time course of protein diffusion into the cell soma appeared to correlate with observed Ca^{2+} buffering effects of these proteins indicating that the proteins were actually responsible for the observed decrease in the peak $[Ca^{2+}]_i$.

The lack of effect of either CABP on the basal $[Ca^{2+}]_i$ is reminiscent of the observations of Baker & Umbach (1987) who found that injecting low concentrations (< 5 mM) of EGTA or BAPTA into squid axoplasm had no effect on the basal $[Ca^{2+}]_i$. This implies that, rather than CABPs, alternative systems such as the Na^+–Ca^{2+} exchanger or Ca^{2+}-ATPase may determine the basal $[Ca^{2+}]_i$. This contention is also supported by other studies on cultured DRG neurones (Benham, Evans & McBain, 1992) which found that the basal $[Ca^{2+}]_i$ was significantly affected by inhibitors of the Ca^{2+}-ATPase but not by perturbation of the Na^+–Ca^{2+} exchanger (see also Thayer & Miller, 1990).

Although neither protein affected the basal $[Ca^{2+}]_i$, both significantly affected depolarization-induced changes in $[Ca^{2+}]_i$ such as the rate of rise of $[Ca^{2+}]_i$, the peak $[Ca^{2+}]_i$ achieved and the rate of decay of $[Ca^{2+}]_i$ from its peak value. The ability of CABPs to buffer Ca^{2+} challenges is dependent not only on their dissociation constants but also on their relative on–off rates (Sala & Hernández-Cruz, 1990; Adler, Augustine, Duffy & Charlton, 1991). *In vitro* analysis of purified forms of both calbindin D_{28k} and parvalbumin have provided information about the kinetics of Ca^{2+} binding. Parvalbumin binds Ca^{2+} with a dissociation constant (K_d) of 1×10^{-7}–1×10^{-8} M in the absence of Mg^{2+} ions (Gillis *et al.* 1982; Hou *et al.* 1991), but due to the competitive binding of Mg^{2+} ($K_d = 1 \times 10^{-4}$), in physiological media

(1 mM Mg^{2+}) the apparent K_d of parvalbumin is approximately 1×10^{-6} to 1×10^{-7} M. In contrast, calbindin D_{28k} has a low affinity for Mg^{2+} ions and an affinity for Ca^{2+} ions of approximately 5×10^{-7} M (Bredderman & Wasserman, 1974). Although the two CABPs have similar apparent K_d values, parvalbumin is likely to be a slower buffer than calbindin D_{28k} since in cells with a typical resting $[Ca^{2+}]_i$ of 1×10^{-7} M, parvalbumin will be 60–90% bound by Mg^{2+} ions (Gillis *et al.* 1982; Hou *et al.* 1991). The Mg^{2+} ions must first dissociate before the protein can begin to bind Ca^{2+} ions. Thus, we would expect parvalbumin to be less effective than calbindin D_{28k} in reducing $d[Ca^{2+}]_i/dt$. Our experimental results support such a contention, since calbindin D_{28k} caused a more pronounced slowing of $d[Ca^{2+}]_i/dt$. The greater effect of calbindin D_{28k} may be attributed to its faster on-rate for Ca^{2+} binding: it buffers influxing Ca^{2+} more rapidly than parvalbumin such that the observed increase in $[Ca^{2+}]_i$ occurs at a slower rate. In fact, theoretical modelling data have suggested that the forward binding constant may be the most significant determinant of the effects of CABPs on $d[Ca^{2+}]_i/dt$ (Nowycky & Pinter, 1993). The slower on-rate for parvalbumin may also be analogous to the properties of EGTA relative to BAPTA. Like calbindin D_{28k} and parvalbumin, EGTA and BAPTA have similar K_ds but BAPTA binds Ca^{2+} ions approximately 400 times faster than EGTA. The faster on-rate is significant when one compares the effects of EGTA and BAPTA on neurotransmitter release. Injection of moderate concentrations of EGTA into presynaptic terminals has no effect on transmitter release whereas injection of BAPTA strongly attenuates it (Adler *et al.* 1991; Augustine, Adler & Charlton, 1991). Studies such as this suggest that because of the different kinetics of Ca^{2+} binding one might expect to see differential effects of calbindin D_{28k} and parvalbumin on Ca^{2+}-dependent processes such as transmitter release.

Ca^{2+} has many important roles to play in the control of neuronal activities in addition to neurotransmitter release. Köhr & Mody (1991) have demonstrated that the induction of epileptiform activity in rats by kindling caused a selective loss of calbindin D_{28k} from dentate granule cells. The Ca^{2+} channels in kindled cells inactivated to a greater extent than control cells. It is thought that the faster rate of channel inactivation is due to a Ca^{2+}-mediated process which is minimized when calbindin D_{28k} is present. However, Lledo *et al.* (1992) transfected calbindin D_{28k} into a pituitary cell line and demonstrated that both T and L type Ca^{2+} currents inactivate more rapidly in the transfected cells than in the wild type cells. Moreover, in the transfected cells both the L and T type current densities were about 50% of those observed in the wild type cell line. In our experiments, analysis of Ca^{2+} current inactivation properties is complicated by the fact that DRG neurones contain a heterogeneous Ca^{2+} channel population (Scroggs & Fox, 1992). Nevertheless, at the concentrations employed, we found that neither calbindin D_{28k} nor parvalbumin had a significant effect on the rate of Ca^{2+} current inactivation (data not shown). Interestingly, when Lledo *et al.* (1992) introduced calbindin D_{28k} into the wild type pituitary cell line via the patch pipette they failed to observe an effect of calbindin D_{28k} on L type Ca^{2+} current activation. We also observed that upon accessing the cell soma, neither protein affected the amplitude of the Ca^{2+} current nor the rate of 'run-down' of the Ca^{2+} current. 'Run-down' may be due to a Ca^{2+}-dependent mechanism (Chad & Eckert, 1986) and may be slowed by addition of EGTA or BAPTA to the

patch pipette. The lack of effect of the two exogenously introduced proteins may be due to an insufficiently high concentration of buffer, due to the buffer not accessing the submembrane Ca^{2+} channel micro-domains, or may be due to insufficiently fast buffering at the channel pore to prevent Ca^{2+}-activated processes. In practice, all three factors may contribute to some extent, since Ca^{2+} would not be expected to be buffered at the channel pore unless a large concentration of a high affinity Ca^{2+} buffer was present in close apposition to the pore (Stern, 1992). It would be necessary that the kinetics of such a Ca^{2+} buffer would only be limited by the time taken for Ca^{2+} to diffuse from the pore. Thus, one may only see an effect of either CABP on Ca^{2+} channel inactivation and 'run-down' at much higher concentrations than those employed in this study. Indeed, the regulation of such processes may not be a physiological role for CABPs.

Although the above events appeared to be unaffected by either protein, other events such as facilitation, which would be influenced by changes in the global $[Ca^{2+}]_i$, could well be altered by the presence of such buffers (Hochner, Parnas & Parnas, 1991). In our study both CABPs reduced the peak global $[Ca^{2+}]_i$. In addition, clear alterations in the time course of the rate of rise and decay of the Ca^{2+} signal were observed. Both proteins slowed the rate of rise of the $[Ca^{2+}]_i$, although calbindin D_{28k} exerted the effect more significantly. Similarly, calbindin D_{28k} slowed the rate of decay of the peak $[Ca^{2+}]_i$ to a much greater extent. The slow decay in $[Ca^{2+}]_i$ from peak values may be a result of calbindin D_{28k} gradually redistributing bound Ca^{2+} to the cellular extrusion apparatus. These observed effects of calbindin D_{28k} agree well with the theoretical predictions of Sala & Hernández-Cruz (1990) for a high affinity Ca^{2+} buffer and with the observations of Lledo *et al.* (1992) who also observed a loss of the fast component of decay in $[Ca^{2+}]_i$ in calbindin D_{28k}-containing cells. Although it has a similar K_d to that of calbindin D_{28k}, parvalbumin caused a characteristic biphasic decay in the peak $[Ca^{2+}]_i$, consisting of a rapid initial decay of the peak $[Ca^{2+}]_i$ followed by a slower second decay phase. The differing effects of parvalbumin on the rise and decay in $[Ca^{2+}]_i$ may be explained by its slower Ca^{2+} binding kinetics. Before parvalbumin can bind influxing Ca^{2+}, it must first wait for bound Mg^{2+} ions to dissociate. As a result, $[Ca^{2+}]_i$ increases more rapidly before the parvalbumin exerts a significant buffering effect. However, parvalbumin may then begin to avidly bind Ca^{2+} ions and this may be observed experimentally, at the end of a depolarizing pulse, as a rapid decay in the Ca^{2+} signal.

The observed Ca^{2+}-buffering properties of parvalbumin are interesting in light of recent observations made by H. E. Scharfman (personal communication; 8th International Symposium on Ca^{2+}-binding Proteins and Ca^{2+} Function in Health and Disease, Davos, Switzerland 1992), who demonstrated that impalement and stimulation of CA3 hippocampal neurones with electrodes containing 100 mM parvalbumin caused pyramidal cells to switch from firing bursts of action potentials to firing trains of action potentials, a pattern more characteristic of hippocampal interneurones than pyramidal cells. The observed effects are presumably due to alterations in the properties of the Ca^{2+}-activated K^+ conductance, which is thought to underlie spike adaptation. One might imagine that a rapid buffering of the $[Ca^{2+}]_i$ by parvalbumin would be required to exert this effect. Whether CABP regulation of $K^+_{(Ca)}$ channel activity occurs physiologically is unknown. However, parvalbumin is

often a marker of fast-firing neurones *in vivo* (Kawaguchi, Katsumaru, Kosaka, Heizmann & Hama, 1987).

Prolonged elevations in $[Ca^{2+}]_i$ disturbs normal cell function and can activate a series of cellular events that results in delayed neuronal cell death. Such Ca^{2+} elevations have been proposed as a common mechanism for the death of neurones observed following seizures and ischaemia (Choi, 1992). Although the hippocampus is particularly vulnerable to the excitotoxic effects of hypoxia and focal epilepsy, within certain subregions the degree of vulnerability varies with some cells showing a high degree of resistance (Sloviter, 1989; Leranth & Ribak, 1991). In these cases, it is thought that the presence or absence of CABPs confers the degree of resistance. For this to be true, the CABPs would have to be able to buffer large Ca^{2+} loads. At the concentrations employed, we found that throughout a range of Ca^{2+} challenges (40–1280 ms) both CABPs were effective in reducing the peak $[Ca^{2+}]_i$ achieved. Similarly, Baker & Schlaepfer (1978) found that axoplasm extruded from axons of *Loligo* and *Myxicola* could buffer concentrations of Ca^{2+} up to 300 μM in an energy-independent manner. The possibility that Ca^{2+} buffering alone is sufficient to prevent cell death has been supported by the demonstration that neurones normally subjected to stimulation-induced degeneration can be rendered resistant by introducing high concentrations of BAPTA into the cell (Scharfman & Schwartzkroin, 1989).

We conclude that both calbindin D_{28k} and parvalbumin can act to buffer $[Ca^{2+}]_i$ in rat sensory neurones, although the characteristics of their buffering properties appear to differ. It will be of interest to compare the buffering properties of these binding proteins to those of newly discovered CABPs such as calretinin (Résibois & Rogers, 1992) and, furthermore, to understand how the heterogeneous subcellular distribution of these proteins can regulate different Ca^{2+}-dependent neuronal functions.

We would like to acknowledge Dr Ning-Sheng Wang for her help with the cell culture, Dr V. P. Bindokas for help with the digital imaging experiments and Dr K. G. Baimbridge for his generous donation of rabbit polyclonal anti-parvalbumin and anti-calbindin D_{28k} antibodies. Also, I would like to thank Ms C. A. Mitchell for her help in preparing the manuscript. This work was supported by grants DA-02121, Mh-40165 and DK-42086 to R.J.M., in part by grants NS20270 and DK28961 to S.C. and by grant PHS NRSA2T32 GMM07151 to P.S.C.

REFERENCES

ADLER, E. M., AUGUSTINE, G. J., DUFFY, S. N. & CHARLTON, M. P. (1991). Alien intracellular calcium chelators attenuate neurotransmitter release at the squid giant synapse. *Journal of Neuroscience* **11**, 1496–1507.

AUGUSTINE, G. J., ADLER, E. M. & CHARLTON, M. P. (1991). The calcium signal for transmitter secretion from presynaptic nerve terminals. In *Calcium Entry and Action at the Presynaptic Nerve Terminal. Annals of the New York Academy of Sciences* **635**, 365–381.

BAIMBRIDGE, K. G., CELIO, M. R. & ROGERS, H. (1992). Calcium-binding proteins in the nervous system. *Trends in Neurosciences* **15**, 303–308.

BAKER, P. F. & SCHLAEPFER, W. W. (1978). Uptake and binding of calcium by axoplasm isolated from giant axons of *Loligo* and *Myxicola*. *Journal of Physiology* **276**, 103–125.

BAKER, P. F. & UMBACH, J. A. (1987). Calcium buffering in axons and axoplasm of *Loligo*. *Journal of Physiology* **383**, 369–394.

BENHAM, C. D., EVANS, M. L. & MCBAIN, C. J. (1992). Ca^{2+} efflux mechanisms following depolarization evoked calcium transients in cultured rat sensory neurones. *Journal of Physiology* **455**, 567–583.

BREDDERMAN, P. J. & WASSERMAN, R. H. (1974). Chemical composition, affinity for calcium, and some related properties of the vitamin D dependent calcium-binding protein. *Biochemistry* **13**, 1687–1694.

CARR, P. A., YAMAMOTO, T., KARMY, G., BAIMBRIDGE, K. G. & NAGY, J. I. (1989). Parvalbumin is highly co-localized with calbindin D_{28k} and rarely with calcitonin gene-related peptide in dorsal root ganglia neurones of rat. *Brain Research* **497**, 163–170.

CELIO, M. R. (1990). Calbindin and parvalbumin in the rat nervous system. *Neuroscience* **35**, 375–475.

CHAD, J. E. & ECKERT, R. (1986). An enzymic mechanism for calcium current inactivation in dialysed *Helix* neurones. *Journal of Physiology* **378**, 31–51.

CHARD, P. S., BLEAKMAN, D. & MILLER, R. J. (1991). Parvalbumin is an intracellular neuronal Ca^{2+} buffering protein. *Society for Neuroscience Abstracts* **17**, 343, 142.12.

CHOI, D. W. (1992). Excitotoxic cell death. *Journal of Neurobiology* **23**, 1261–1276.

FABATIO, A. & FABATIO, F. (1979). Calculator programs for computing the composition of solutions containing metals and ligands used for experiments in skinned muscle cells. *Journal de Physiologie* **75**, 463–505.

GILLIS, J. M., THOMASON, D., LEFEVRE, J. & KRETSINGER, R. H. (1982). Parvalbumins and muscle relaxation: a computer simulation study. *Journal of Muscle Research and Cell Motility* **3**, 377–398.

GRYNKIEWICZ, G., POENIE, M. & TSIEN, R. Y. (1985). A new generation of calcium indicators with greatly improved fluorescence properties. *Journal of Biological Chemistry* **260**, 3440–3450.

HAMILL, O. P., MARTY, A., NEHER, E., SAKMANN, B. & SIGWORTH, F. J. (1981). Improved patch clamp technique for high resolution current recording from cells and cell free membrane patches. *Pflügers Archiv* **391**, 85–100.

HEIZMANN, C. W. & HUNZIKER, W. (1991). Intracellular calcium-binding proteins: more sights than insights. *Trends in Biochemical Sciences* **16**, 98–103.

HOCHNER, B., PARNAS, H. & PARNAS, I. (1991). Effects of intra-axonal injection of calcium buffers on evoked release and on facilitation in the crayfish neuromuscular junction. *Neuroscience Letters* **125**, 215–218.

HOU, T.-T., JOHNSON, J. D. & RALL, J. A. (1991). Parvalbumin content and calcium and magnesium dissociation rates correlated with changes in relaxation rate of frog muscle fibres. *Journal of Physiology* **441**, 285–304.

JONES, S. W. & MARKS, T. N. (1989). Ca^{2+}-currents in bullfrog sympathetic neurones. II. Inactivation. *Journal of General Physiology* **94**, 169–182.

KAWAGUCHI, Y., KATSUMARU, H., KOSAKA, T., HEIZMANN, C. W. & HAMA, K. (1987). Fast-spiking neurones in rat hippocampus (CA1 region) contain the calcium-binding protein parvalbumin. *Brain Research* **416**, 369–374.

KELLOG, D. R., MITCHISON, T. J. & ALBERTS, B. M. (1988). Behavior of microtubules and actin filaments in living Drosophila embryos. *Development* **103**, 675–686.

KÖHR, G. & MODY, I. (1991). Endogenous intracellular calcium buffering and the activation/inactivation of HVA calcium currents in rat dentate gyrus granule cells. *Journal of General Physiology* **98**, 941–967.

KOSAKA, T., KOSAKA, K., NAKAYAMA, T., HUNZIKER, W. & HEIZMANN, C. W. (1993). Axons and axon terminals of cerebellar purkinje cells and basket cells have higher levels of parvalbumin immunoreactivity than somata and dendrites: quantitative analysis by immunogold labelling. *Experimental Brain Research* **93**, 483–491.

KRETSINGER, R. H. & NOCKOLDS, C. E. (1973). Carp muscle calcium-binding protein. II. Structure determination and general description. *Journal of Biological Chemistry* **248**, 3313–3326.

LERANTH, C. & RIBAK, C. E. (1991). Calcium-binding proteins are concentrated in the CA2 field of the monkey hippocampus: a possible key to this region's resistance to epileptic damage. *Experimental Brain Research* **85**, 129–136.

LLEDO, P. M., SOMASUNDARAM, B., MORTON, A. J., EMSON, P. C. & MASON, W. T. (1992). Stable transfection of calbindin D28k into the GH3 cell line alters Ca^{2+} currents and intracellular Ca^{2+} homeostasis. *Neuron* **9**, 943–954.

MATTSON, M. P., RYCHLIK, C. C., CHU, C. & CHRISTAKOS, S. (1991). Evidence for calcium-reducing and excitoprotective roles for the calcium-binding protein calbindin D_{28k} in cultured hippocampal neurones. *Neuron* **6**, 41–51.

NOWYCKY, M. C. & PINTER, M. J. (1993). Time courses of calcium and calcium-bound buffers following calcium influx in a model cell. *Biophysical Journal* **64**, 77–91.

OBERHOLTZER, J. C., BUETTGER, C., SUMMERS, M. C. & MATSCHINSKY, F. M. (1988). The 28-kDa calbindin-D is a major calcium-binding protein in the basilar papilla of the chick. *Proceedings of the National Academy of Sciences of the USA* **85**, 3387–3390.

POCHET, R., LAWSON, D. E. M. & HEIZMANN, C. W. (1990). Calcium-binding proteins in normal and transformed cells. *Advances in Experimental Medicine and Biology* **269**, 1–223.

PUSCH, M. & NEHER, E. (1988). Rates of diffusional exchange between small cells and a measuring patch pipette. *Pflügers Archiv* **411**, 204–211.

RÉSIBOIS, A. & ROGERS, J. H. (1992). Calretinin in rat brain: an immunohistochemical study. *Neuroscience* **46**, 101–134.

SALA, F. & HERNÁNDEZ-CRUZ, A. (1990). Calcium diffusion modelling in a spherical neurone. Relevance of buffering properties. *Biophysical Journal* **57**, 313–324.

SCHARFMAN, H. E. & SCHWARTZKROIN, P. A. (1989). Protection of dentate hilar cells from prolonged stimulation by intracellular calcium chelation. *Science* **246**, 257–260.

SCROGGS, R. S. & FOX, A. P. (1992). Calcium current variation between acutely isolated adult rat dorsal root ganglion neurones of different size. *Journal of Physiology* **445**, 639–658.

SLOVITER, R. S. (1989). Calcium-binding protein (calbindin-D 28k) and parvalbumin immunohistochemistry: Localization in the rat hippocampus with specific reference to the selective vulnerability of hippocampal neurones to seizure activity. *Journal of Comparative Neurology* **280**, 183–196.

STERN, M. D. (1992). Buffering of calcium in the vicinity of a channel pore. *Cell Calcium* **13**, 183–192.

THAYER, S. A. & MILLER, R. J. (1990). Regulation of the intracellular free calcium concentration in single rat dorsal root ganglion neurones *in vitro*. *Journal of Physiology* **425**, 85–115.

THAYER, S. A., PERNEY, T. M. & MILLER, R. J. (1988*a*). Regulation of Ca^{2+} homeostasis in sensory neurones by bradykinin. *Journal of Neuroscience* **8**, 4089–4097.

THAYER, S. A., STUREK, M. & MILLER, R. J. (1988*b*). Measurement of neuronal Ca^{2+} transients using simultaneous microfluorimetry and electrophysiology. *Pflügers Archiv* **412**, 216–223.

WASSERMAN, R. H. & TAYLOR, A. N. (1966). Vitamin D3-induced calcium-binding protein in chick intestinal mucosa. *Science* **152**, 791–793.